Proceedings of the 17th World Congress
The International Federation of Automatic Control
Seoul, Korea, July 6-11, 2008

Design Methodology for Robust and Fault-Tolerant Control of a Microprehensile Microrobot-On-Chip

Moussa Boukhnifer, Antoine Ferreira, Frédéric Kratz

PRISME Institute, ENSI de Bourges, Bourges, France.
(Tel: +332 4848 4079; e-mail: antoine.ferreira@ensi-bourges.fr).

Abstract: Recently, the evolution of microfabrication technologies and component integration at microscale led to the development of integrated Microrobot-On-Chip (MOC) where on-chip control refers to integrated miniaturized systems where the control algorithms, sensors and actuators are included as part of the system. Enabling these types of micromechatronic systems requires research in methods to deal with sensor and actuator robustness with fault-tolerant control against micromechanical failures, microphysical uncertainties (adhesive effects, object repulsion/attraction) and noise spikes in sensing instruments. This paper presents a general architecture for fault tolerant control using Youla parametrization for a piezoelectric microrobotic gripper. The distinguished feature of our controller architecture is that it shows structurally how the controller design for performance and robustness may be done separately which has the potential to overcome the conflict between performance and robustness in the traditional feedback framework. The controller architecture includes two parts: one part for performance and the other part for robustness. The controller architecture works in such a way that the feedback control system will be solely controlled by the PI performance controller for a nominal model and the H_∞ robustification controller will only be active in the presence of the uncertainties or external disturbances.

1. INTRODUCTION

Actually, the automation of basic microrobotic tasks for manipulation, gripping and assembly of microparts is the main challenge in MEMS, NOEMS and microsystem industry. As more microrobotic manipulation operations become more and more automated, the need for robustness towards system faults, external disturbances or sensor noise increased. As example, when a microrobotic gripper is handling hazardous microparts due to the influence of near-field adhesive microforces (van der Waals, capillary, electrostatics) [1] or performing critical tasks with a high risk of failure (*i.e.*, cell injection, gene handling) [2], a good fault tolerant control (FTC) is required. Sensor's faults affect the system's performance in the closed-loop system when the faulty microsensor is used to control the input. However, even if there is a scheme to detect the fault, due to the nature and confined space of micromanipulation, it might not be feasible to intervene and rectify the problem safely in a timely way. Face to the external mechanical disturbances occurring during microrobotic operations a high degree of robustness with good performances is also required [3], [4].

There has been a lot of work made on FTC for macroscopic robotics. Goel *et al.* [5] presented a FTC method for a teleoperated multi-link manipulator subjected to locked joint failures. Izumikawa *et al.* [6] proposed a flexible joint FTC scheme for sensor faults; when a certain sensor fails, the feedback control scheme changes gains in order to not let the system performance degrade too much. The FTC scheme proposed by Tan et Habib [7] consists mainly of a fault reconstruction scheme where the outputs are firstly separated into non-faulty and potentially faulty actuator-sensor components. However, it should be mentioned as far as we know, several works have been reported for robust control of microactuation systems, *i.e.*, electromagnetic [8], piezoelectric [9] and magnetostrictive [10] driving systems but few works reported fault tolerant control in micro and nanorobotics [11]. The results of this work relates to the areas of fault tolerant control and robust control for a microrobotic piezoelectric microgripper.

This paper presents a general architecture for fault tolerant control using Youla parametrization for a piezoelectric microgripper. The distinguished feature of our controller architecture is that it shows structurally how the controller design for performance and robustness may be done separately which has the potential to overcome the conflict between performance and robustness in the traditional feedback framework. When a sensor fails or degrades, the controller switches and uses the observer's output instead of the original system's output. The controller architecture includes two parts: one part for performance and the other part for robustness. The controller architecture works in such a way that the feedback control system will be solely controlled by the PI performance controller for a nominal model and the H_∞ robustification controller will only be active in the presence of the uncertainties or external disturbances.

The paper can be summarized as follows. In section 2, we recall the standard Youla parametrization before to introduce the proposed FTC control architecture in section 3. Then, section 4 presents the simulation and

experimental results without and with the proposed robust FTC controller when subjected to external perturbations and faulty sensor operation.

2. THE YOULA PARAMETRIZATION

Before considering the FTC design, the Youla parametrization is shortly introduced. The controller architecture applied for the FTC in the following will be based on the Youla parametrization. It should be noticed that the Youla parametrization has also been applied in connection with FTC in similar works presented in [12],[13].

Consider in Fig.1 the following general control scheme where P is nominal system controlled by the controller K:

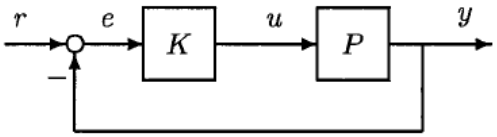

Fig. 1. Controller K.

Let a coprime factorization of the system P and a stabilizing controller K be given by:

$$\begin{aligned} P &= N_u M^{-1} = \tilde{M}^{-1}\tilde{N}_u, \quad N_u, M, \tilde{N}_u, \tilde{M} \in \Re H_\infty \\ K &= UV^{-1} = \tilde{V}^{-1}\tilde{U}, \qquad U, V, \tilde{U}, \tilde{V} \in \Re H_\infty \end{aligned} \tag{1}$$

where the eight matrices in (1) must satisfy the double Bezout equation given by (see [14] for details):

$$\begin{pmatrix} I & 0 \\ 0 & I \end{pmatrix} = \begin{pmatrix} \tilde{V} & -\tilde{U} \\ -\tilde{N}_u & \tilde{M} \end{pmatrix} \begin{pmatrix} M & U \\ N_u & V \end{pmatrix} \tag{2}$$

$$= \begin{pmatrix} M & U \\ N_u & V \end{pmatrix} \begin{pmatrix} \tilde{V} & -\tilde{U} \\ -\tilde{N}_u & \tilde{M} \end{pmatrix} \tag{3}$$

Based on the above coprime factorization of the system $G(s)$ and the controller $K(s)$, we can give a parametrization of all controllers that stabilize the system in terms of a stable parameter $Q(s)$, i.e. all stabilizing controllers are given by [15]:

$$K(Q) = U(Q)V(Q)^{-1} \tag{4}$$

where

$$U(Q) = U + MQ, V(Q) = V + N_u Q, \quad Q \in \Re H_\infty \tag{5}$$

or by using a left factored form:

$$K(Q) = \tilde{V}(Q)^{-1}\tilde{U}(Q) \tag{6}$$

where

$$\tilde{U}(Q) = \tilde{U} + Q\tilde{M}, \tilde{V}(Q) = \tilde{V} + Q\tilde{N}_u, \quad Q \in \Re H_\infty \tag{7}$$

Using the Bezout equation, the controller given either by (5) or by (7) can be realized as a LFT (Linear Fractional Transformation) in the parameter Q,

$$K(Q) = F_l(J_K, Q) \tag{8}$$

where J_K is given by:

$$J_k = \begin{pmatrix} UV^{-1} & \tilde{V}^{-1} \\ V^{-1} & -V^{-1}N_u \end{pmatrix} = \begin{pmatrix} \tilde{V}^{-1}\tilde{U} & \tilde{V}^{-1} \\ V^{-1} & -V^{-1}N_u \end{pmatrix} \tag{9}$$

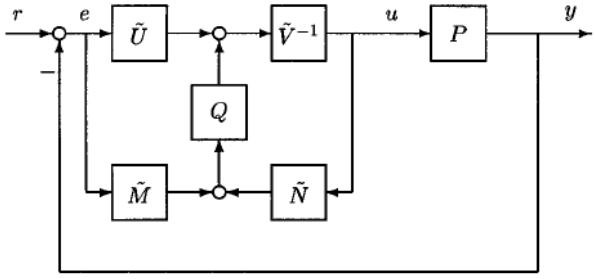

Fig. 2. Controller structure with parametrization.

Reorganizing the controller $K(Q)$ given by 9 results in the closed-loop system depicted in Fig.2, [15].

3. FTC CONTROLLER ARCHITECTURE

In this section, we use the Youla parametrization in a non-traditional way (as shown in Fig.2) and we explain how to use this architecture in order to ensure both performance and robustness outcomes.

Firstly, we consider the feedback diagram presented in Fig.3. This is not equivalent to the diagram in Fig.2 since the reference signal r enters into the system from a different location. Nevertheless, the internal stability of the system is not changed since the transfer function from y to u is not changed. Thus, this controller implementation also stabilizes internally the feedback system with plant P_0 for any $Q \in H_\infty$ such that $\det(\tilde{V}(\infty) - Q(\infty)\tilde{N}(\infty)) \neq 0$.

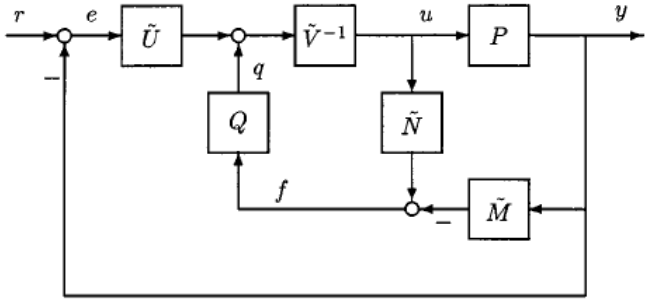

Fig. 3. GIMC structure

Due to the similarity with the well-known IMC (Internal Model Control), see [16] for details, we shall call our controller framework as generalized internal model control (GIMC) [18].

The distinguished feature of this controller implementation is that the inner loop feedback signal f is always zero, i.e., $f = 0$, if the plant model is perfect, i.e., if $P = P_0$. The inner loop is only active when there is a model uncertainty or other sources of uncertainties such as disturbances and sensor noises. Thus, Q can be designed to robustify the feedback system. It follows that the new controller design architecture has a clear separation between performance and robustness.

4. CONTROLLER DESIGN

A high performance robust system can be designed in two steps:

(1) Design $K_0 = \tilde{V}^{-1}\tilde{U}$ to satisfy the system performance specifications with a nominal plant model P_0;
(2) Design Q to satisfy the system robustness requirements. Note that the controller Q will not affect the system nominal performance.

It should be emphasized that K_0 is not just any stabilizing controller as in most of controller parameterizations used in the literature, it is designed to satisfy certain performance specifications. For example, K_0 may be a simple PI controller:

$$K_0 = \frac{K_p(s+a)}{s} \tag{10}$$

that satisfies our design specifications, in which case we can take $\tilde{U} = 1$ and $\tilde{V} = K_0 = \frac{K_p(s+a)}{s}$.

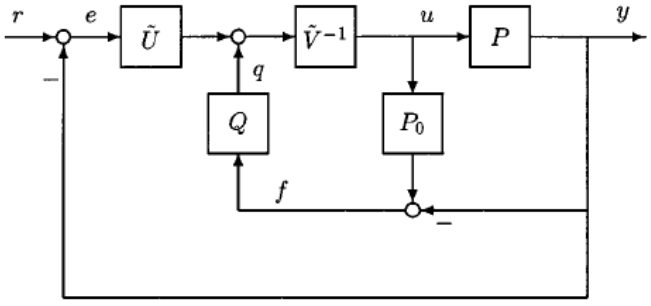

Fig. 4. Alternative structure of GIMC [18].

The output error f defined in Fig.4 is the residual signal. In the fault diagnosis literature, f is used to detect the possible faults in actuator and/or sensors. If $f = 0$, we have not a fault but if $f = 1$ a robust controller is implemented using the standard feedback structure shown in Fig.1. The fault-tolerant controllers can be designed such that they provide adequate performance when there are no faults in the systems and as much tolerance as possible by any other fault-tolerant or robust controllers.

Such controllers can be designed in two steps:

(1) Design $K_0 = \tilde{V}^{-1}\tilde{U}$ to satisfy the performance for a nominal system;
(2) Design Q to tolerate possible actuators and/or sensors failures (and model uncertainties). This Q can be using standard robust control technique, fuzzy control, sliding mode control, etc. In our case, we use the robust H_∞ technique.

5. ROBUSTIFICATION

In this section, we shall consider how to design the controller K for a high degree of system robustness.

Consider the system described by the block diagram of the Fig.5,

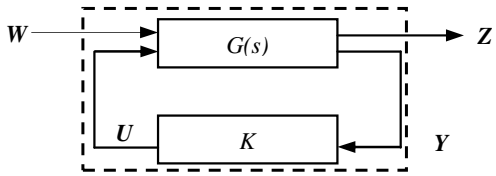

Fig. 5. H_∞ robust control.

where P is the generalized plant and K is the controller. Only finite-dimensional linear time invariant (LTI) systems and controllers will be considered in this paper. The generalized plant P contains what is usually called the plant in a control problem plus all weighing functions. The signal w contains all external inputs, including disturbances, sensor noise, and commands; the output z is an error signal; y is the measured variables; u is the control input. The diagram is also referred to as a linear fractional transformation (LFT) on K, and P is called the coefficient matrix for the LFT. The resulting closed-loop transfer function from w to z is denoted by T_{zw}. The problem of H_∞ standard is to synthesize a controller K which stabilizes the system P and minimize the norm H_∞ of T_{zw} [17].

$$P = \begin{bmatrix} A & B_1 & B_2 \\ C_1 & 0 & D_{12} \\ C_2 & D_{21} & 0 \end{bmatrix} \tag{11}$$

The following assumptions are made:

(1) (A, B_1) is stabilizable and (C_1, A) is detectable.
(2) (A, B_2) is stabilizable and (C_2, A) is detectable.
(3) $D_{12}'[C_1 \quad D_{12}] = [0 \quad I]$.
(4) $[B_1 \quad D_{21}]^T D_{21}' = [0 \quad I]^T$.

The problem of H_∞ standard is to synthesize a controller K which stabilizes the system G and minimize the H_∞ norm of $\| T_{zw} \|_\infty$.

Recall that the H_∞ controller is :

$$K_\infty = \begin{bmatrix} \hat{A}_\infty \mid -Z_\infty L_\infty \\ F_\infty \quad\quad 0 \end{bmatrix} \tag{12}$$

$\hat{A} = A + \gamma^{-2} B_1 B_1' X_\infty + B_2 F_\infty C_2$.
$F_\infty = -B_2' X_\infty,\ L = -Y_\infty C_2,\ Z_\infty = (I - \gamma^{-2} Y_\infty X_\infty)^{-1}$.

where $X_\infty = Ric(H_\infty)$ and $Y_\infty = Ric(J_\infty)$ the necessary and sufficient conditions for the existence of an admissible controller such that of $\| T_{zw} \|_\infty < \gamma$ are as follows:

(1) $H_\infty \in$ dom(Ric) and $X_\infty = Ric(H_\infty \geq 0$.
(2) $J_\infty \in$ dom(Ric) and $X_\infty = Ric(H_\infty \geq 0$.
(3) $\rho(X_\infty Y_\infty) < \gamma^2$

where Ric stands for the standard solution of Ricatti equation.
The Hamiltonian matrices are defined as:

$$H_\infty = \begin{bmatrix} A & \gamma^{-2} B_1 B_1^T - B_2 B_2^T \\ -C_1^T C_1 & -A^T \end{bmatrix} \tag{13}$$

$$J_\infty = \begin{bmatrix} A^T & \gamma^{-2}C_1C_1^T - C_2^TC_2 \\ -B_1B_1^T & -A \end{bmatrix} \quad (14)$$

The fault tolerant control problem depends strongly on the type of faults that can appear in the system. In this paper, the faults are described as *additive faults*. In connection with FTC, this might not be very useful. The reason is that the additive faults can be considered as external input signals to the system which will not cause any changes in the system dynamics. Specifically, they are not able to change the stability of the closed-loop system but the performance of the system will be affected. The controller Q can be designed using the standard robust techniques as shown in Fig.6, where Δ include the additive fault.

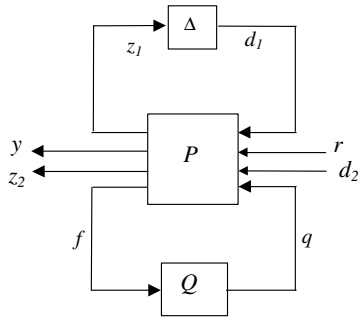

Fig. 6. The standard setup for design of Q for systems with additive faults.

The H_∞ design of Q may be carried as per Fig.6 such as:

$$z = \begin{bmatrix} W_1(r-y) \\ W_2u \end{bmatrix} \quad , \; w = \begin{bmatrix} r \\ d_1 \\ d_2 \end{bmatrix}$$
$$y = \begin{bmatrix} r + W_3d_1 \\ y + W_4d_2 \end{bmatrix} \quad , \quad u = u_s \quad (15)$$

6. SIMULATIONS AND EXPERIMENTS

6.1 Identification of the system

Figure 7.(a) shows the micromanipulator with the four-degree-of-freedom (4-DOFs) microgripper used in the experiments. It is called MMOC (Microprehensile Microrobot-On-Chip) and has been developed at the Laboratoire d'Automatique of Besançon, France [19] operating under the field of view of an optical microscope. Thus the fingers are made from a monolithic micromachining approach since the microgripper, structure and actuators are built of the same piezoelectric zirconate titanate substrate. Each finger is constituted by a piezoelectric bimorph which is deflected in out-of-plane (z-axis) and/or in-plane (y-axis) directions in the bending mode. The proposed control algorithms are designed under the assumption that the environmental force in microenvironment is measurable but due to small size of the microgripper, it is difficult to incorporate strain gauges force sensors at the tip and scaling process amplifies greatly sensor noises to unacceptable

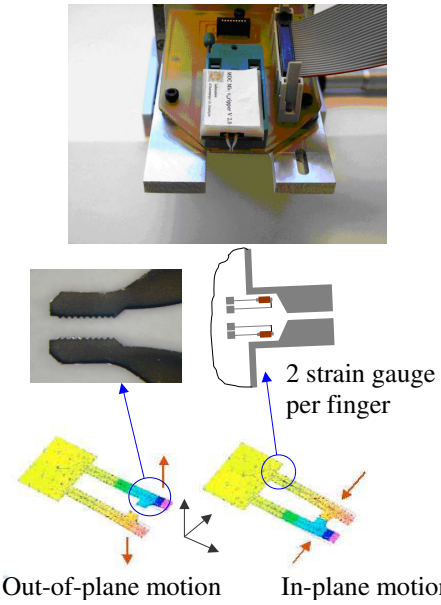

Fig. 7. Microprehensile Microrobot-On-Chip (MOC). (a) Structure of the two-fingered microprehensile MOC and (b) force sensorized end-effectors structure.

level. The solution we selected consisted in using remote-located sensors, such as strain gauges, glued in the position of maximum strain of the gripper, as previously identified by FEM analysis (Fig.7.(b)). A semiconductor strain gauge (type ESB-020-500 from Entran Devices) was glued to the flexure joint at both sides of the monolithic piezoelectric fingers. Sensor calibration for the bridge strain gauge is essential to determine the references of gripping force and tip displacement. In the first part, we measured the displacement of the force variation. Simultaneously, the signal of the strain gauge was measured to obtain the relationship between strain and displacement of the microgripper tip. The force sensor was calibrated by pushing the microgripper tip against the load cell (full scale: $100mN$, resolution: $0.05mN$). The slope of gripping force signal to strain gauge signal was approximately $78\mu N/V$. The force sensibility is less than one milliNewton. Considering the statistics of calibration data, the maximum errors fitting line and data are $0.23V$ in position sensor and $0.45V$ in force sensor. The microgripper is currently attached to a xyz micropositioning system.

The modeling of the device was done using the Bode identification technique where a specific point in the operating range of the device was chosen (where its behavior is approximately linear). A model of the device at this point has been identified by studying its frequency response over a prespecified bandwidth. For this purpose, we used a series of sinusoidal inputs, $V = 10sin(2\Pi ft)$, with frequencies spanning a bandwidth of $1kHz$. The position is sensed by a high-precision linear displacement microsensor ($LVDT$) with a resolution of $1\mu m$. The frequency response of the device at this operating point is shown by the Bode diagram in Fig.8.

$$G(s) = \frac{0.02.10^{-5}}{2.05.10^{-3}s^2 + 2.15.10^{-2}s + 1} \quad (16)$$

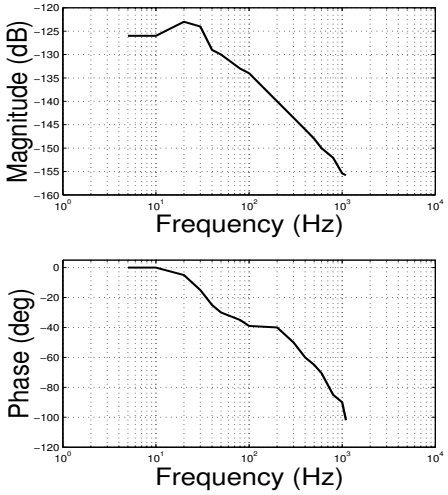

Fig. 8. Frequency responses of the plant G.

6.2 Characterization of the Microrobot-On-Chip

In this section, the MOC microgripper is characterized in terms of range, sensitivity and resolution in the open- and closed-loop configurations. The calibration data showed some hysteresis in open-loop. Hysteresis is primarily due to the nonlinear relationship between applied voltage and finger displacement which are important for large finger deflections. To present the effectiveness of the H_∞ closed-loop design, the hysteresis curves obtained in open-loop (Fig.9(a)) are compared with the closed-loop design (Fig.9(b)). We can see clearly in (Fig.9(a)) that for a finger deflection of 20μm, a maximum output hysteresis of 6.5μm (26%) was observed. The same experiment with the closed-loop controller showed that the effects were practically eliminated (Fig.9(b)). An important observation comes from the fact that the operating applied voltage is settled to $100V$ while the system was identified for a low value of input signal (settled to $5V$). It shows clearly the linearity relationship between the input-output signals. Similar linearity results have been measured when considering creep effects. It should be noticed that important variations were observed for different fingers displacement over a range of $100\mu m$.

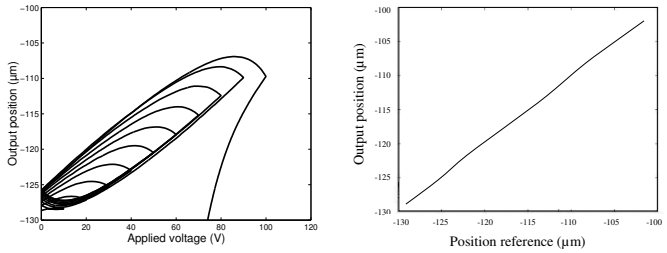

(a) (b)

Fig. 9. (a) Hysteretic behavior for one piezoelectric finger and (b) the H_∞ controller to remove the hysteresis.

6.3 FTC Control

In the sequel, an architecture for fault tolerant controller has been proposed, based on the GIMC structure shown in the block diagram in Fig.4. There is a number of reasons for using the architecture from the Youla parametrization in connection with FTC. Using this architecture, the Q parameter will be the FTC part of the controller. This means that the FTC part of the feedback controller is a modification of the existing controller. Thus, a controller change when a fault appears in the system is not a complete shift to another controller, but only a modification of the existing controller by adding a correction signal in the nominal controller, the r signal in Fig.4. In short terms, we use the PI controller for the ideal model and the H_∞ controller in the presence of the fault. The simulation result given in the Fig.10 shows the ideal response of our system using PI controller.

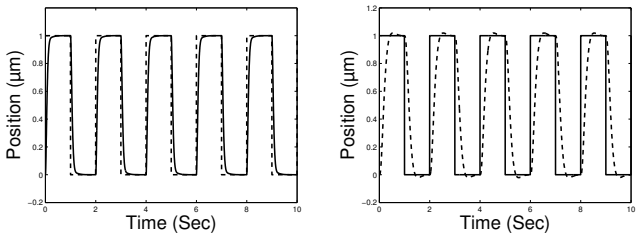

(a) (b)

Fig. 10. Position response with (a) PI controller and (b) H_∞ controller.

For the H_∞ controller design, the specifications are taken to ensure the position should track the reference position. The control U should not exceed a prespecified saturation limit and rejects the fault. It ensures $\| f(G,Q) \|_\infty < \gamma$ for all $\|\Delta\|_\infty < 1$. The controller synthesis is based on the equation (15) where the weighting matrices are chosen as follows:

$$w_1 = 0.019\frac{s^2+10s+10000}{s^2+10s+0.1}, \quad w_2 = 0.5\frac{s}{s+1000},$$

$$w_3 = 0.01\frac{s}{0.001s+1}, \quad w_4 = 1.$$

As illustration of the robustness of the controller, the fault is given as a normally Gaussian distributed random signal with 10 mean value and a variance at 50 as shown in Fig.11. In practice, the fault is induced by a vibratory external mechanical constraint applied to a microgripper finger (random microforce as perturbation). Simulation results show the response of our system using PI and H_∞ controllers. For FTC architecture, the system has been simulated with a reference step at $t = 2sec$ and a fault actuator appeared at $t = 5sec$. The result of the simulation is shown in figure 12(a). It can be seen directly from this figure that the faulty closed-loop system is unstable. For stabilizing the faulty servo system a Q controller needs to be included. As calculated above, the robust controller Q can be applied for stabilizing the faulty closed-loop system. In this example, the Q controller will be implemented with a switching system. Based on the design of Q, the step response of the microgripper is shown in Fig.12(b) where it should be noticed that the standard robust controller is independent of the nominal controller PI. In the worst case, our controller implementation will be equivalent to the existing robust control design. Similar results of robustness and fault-tolerance are obtained when considering faults produced by mechanical contacts due to attraction of the fingers (adhesive forces) or noisy sensing

signals provided by the strain gauge force microsensors during micromanipulation tasks.

Of course, if there is no uncertainty, our controller will perform as well as a nominal controller does. In fact, our framework provides a great flexibility in controller design, for example, one could still use all the robust and H_∞ design techniques here. All one has to do is to start with a good performance controller and then everything can proceed as in the standard robust control design procedure to find the robust controller Q. The only difference is that we are not interested in plugging Q into the controller parametrization to find the total controller rather we will implement the performance controller and the robust controller Q separately.

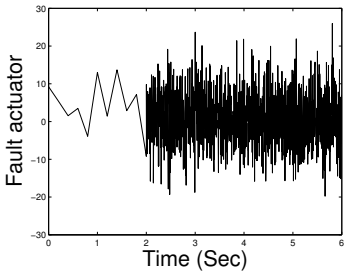

Fig. 11. Faulty actuator.

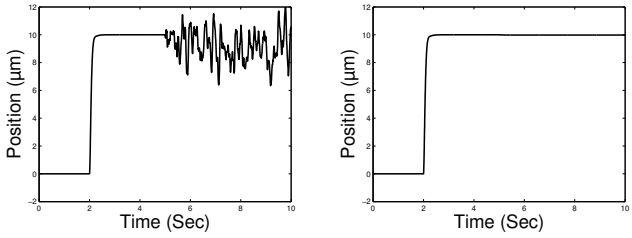

(a) (b)

Fig. 12. Step responses of the microgripper with (a) a fault actuator and (b) using FTC feedback.

7. CONCLUSION

In this paper, an architecture for fault tolerant control has been used for driving in closed-loop a piezoelectric microrobotic gripper. By applying the GIMC structure, an additional controller parameter has been introduced as the main tool to achieve fault tolerance. A feature of the GIMC structure is that it automatically includes a diagnostic signal. The presented simulation and experimental results show that the GIMC provide adequate performance when there are no faults in the system and a tolerance by H_∞ robust controller. In the future work, we will integrate the controller architecture into the MOC chip for a fault-tolerant on-board microrobotic system.

REFERENCES

[1] A. Ferreira, C. Cassier, S. Hirai, Automated Microassembly System Assisted by Vision Servoing and Virtual Reality, *IEEE Trans. on Mechatronics*, Vol. 9, No.2, June 2004, 321-333.

[2] Y. Sun and B. J. Nelson, Microrobotic Cell Injection, *IEEE ICRA*, Seoul, Korea, 2001, 620-625.

[3] Chen, J., Patton, R.J., "Robust model-based fault diagnosis for dynamic systems", *Kluwer Academic Publishers*, 1999.

[4] Edwards, C., Tan, C.P. "Fault tolerant control using sliding mode observers", *Control Engineering Practice*, Vol.14, 2006, pp.897-908.

[5] Goel, M., Maciejewski, A.A., Balakrishan, V. "Failure tolerant teleoperation of a kinematically redundant manipulator: an experimental study", *IEEE Trans. on Systems, Man and Cybernetics -Part A*, Vol.33, 2003, pp.758-765.

[6] Izumikawa, Y., Yubai, K., Hori, T. "Vibration suppression control of a flexible arm robot by PD gain switching sensor failure", *IEEE Int. Conf. on Industrial technology*, Thailand, 2002, pp.684-689.

[7] Tan, C.P., Habib, M.K. "Tolerance towards sensor faults: An application to a flexible arm manipulator", *J. of Advanced Robotic Systems*, Vol.3, N.4, 2006, pp.343-350.

[8] Odgach, P.F. Stoustrup, J., Andersen, P., Wieckerhauser, M.V. "Feature based handling of surface faults in compact disc players", 6^{th} *ECC*.

[9] Liaw H.C., Shirinzadeh, P., Smith J., "Robust adaptive motion tracking control of piezoelectric actuation systems for micro/nano manipulation", *IEEE ICRA*, Roma, Italy, 2007.

[10] Nealis, J.M., Smith, R.C., "Model-based robust control design for magnetostrictive transducers operating in hysteretic and nonlinear regimes", *IEEE Trans. on Control Systems Technology*, Vol.15, N.1, Jan. 2007, pp.22-39.

[11] Hollinger, G.H., Gwaltney, D.A. , "Evolutionary design of fault-tolerant analog control for a piezoelectric pipe-crawling microrobot", *8th annual Conf. on Genetic and Evolutionary computation*, Washington, 2006, pp.761-768.

[12] Stoustrup, J. and Niemann, H.,"Fault tolerant feedback control using the youla parametrization", 6^{th} *ECC*, Portugal, Sept. 2001, pp. 19701974.

[13] Zhou, K. and Ren, Z., "A new controller architecture for high performance robust, and fault-tolerant control", *IEEE Trans. on Automatic Control*, Vol. 46(10), 2001, pp. 16131618.

[14] Zhou, K., Doyle, J., and Glover, K., "Robust and optimal control", Prentice Hall, 1995.

[15] Tay, T., Mareels, I., and Moore, J., "High performance control", Birkhauser, 1997.

[16] M. Morari and E. Zafiriou, "Robust Process Control". Upper Saddle River, NJ: Prentice-Hall, 1989.

[17] J. Doyle, K. Glover, P. Khargonekar, and B. Francis, "State-space solutions to standard H_2 and H_∞ control problems", *IEEE Trans. on Automatic Control*, AC-34, no. 8, pp. 831-847, Aug. 1989.

[18] K Zhou, Z Ren,"A new controller architecture for high performance, robust, and fault-tolerant control", *IEEE Trans. on Automatic Control*, vol. 46, NO. 10, October 2001.

[19] A. Ferreira, J. Agnus, N. Chaillet, J.M. Breguet, "A Smart Microrobot On Chip: Design, Identification and Control", *IEEE Trans. on Mechatronics*, Vol.9, No.3, September 2004, pp.508-519.